Chemical Science

ROYAL SOCIETY OF CHEMISTRY

EDGE ARTICLE

View Article Online
View Journal | View Issue

Cite this: *Chem. Sci.*, 2024, **15**, 12388

All publication charges for this article have been paid for by the Royal Society of Chemistry

Received 26th April 2024
Accepted 29th June 2024

DOI: 10.1039/d4sc02788d

rsc.li/chemical-science

Mixed host co-assembled systems for broad-scope analyte sensing†

Allison J. Selinger, ‡[ab] Joana Krämer, ‡[abc] Eric Poarch, [d] Dennis Hore, [ad] Frank Biedermann *[c] and Fraser Hof *[ab]

Here we report a systems chemistry oriented approach for developing information-rich mixed host chemosensors. We show that co-assembling macrocyclic hosts from different classes, DimerDye sulfonatocalix[4]arenes and cucurbit[*n*]urils, effectively increases the scope of analyte binding interactions and therefore, sensory outputs. This simple dynamic strategy exploits cross-reactive noncovalent host–host complexation interactions while integrating a reporter dye, thereby producing emergent photophysical responses when an analyte interacts with either host. We first demonstrate the advantages of mixed host co-assembled chemosensors through an increased detection range of hydrophobic, cationic, neutral, and anionic drugs. We then implement mixed host sensors in an array-based platform for the differentiation of illicit drugs, including cannabinoids, benzodiazepine analogs, opiates, anesthetics, amphetamine, and common adulterating substances. Finally, the potential of this approach is applied to profiling real-world multi-component illicit street drug samples, proving to be more effective than classical sensor arrays.

Introduction

Synthetic receptors are a powerful tool for molecular recognition-based sensing. Chemosensors have a broad range of applications, such as the detection of biorelevant compounds for diagnostics, and monitoring biophysical and enzymatic processes.[1,2] An ultimate goal for synthetic sensors is to mimic the human olfactory system, containing the ability to identify many different entities from a single sensory tool.[3,4] More recently, the conceptual development of sensors has advanced towards information-rich chemical nose or cross-reactive chemosensors to achieve more prolific unique sensing profiles. This is done through either synthetic design or supramolecular assembly, combining multiple receptor and/or reporter elements into one sensing unit.[3,5] These design strategies are highlighted by examples of unimolecular probes that covalently integrate multiple complexing receptor and/or reporter components,[6,7] and biological non-covalent self-assembly-based probes that function through multi-complexing systems.[8–11]

Macrocyclic hosts are well-defined synthetic receptors for the detection of small molecules and biomacromolecules.[12–14] Host-based sensing is traditionally done using an indicator displacement assay (IDA) that operates through competitive binding of an analyte to a preformed host-indicator complex. This generally results in a fluorescence response, where sensitivity is dictated by binding affinity.[15–17] Singular host sensing systems provide limited information, typically in the form of a single output (turn-on or turn-off fluorescence) for one particular class of analyte and often fail to achieve specificity when faced with structurally similar analytes. To attain analyte differentiation a suite of individual host-indicator sensors are often applied, where varied response patterns arise from affinity differences, producing an optical fingerprint for discrimination.[18] This strategy has been employed in macrocyclic host-based sensor arrays with some recent examples in differentiating neurotransmitters,[19] small molecule bioorganic analytes,[20] folded DNA G-quadruplexes,[21–23] insect pheromones,[24] natural amino acids,[25] and amyloid structures.[26]

The power of increasing cross-reactive self-assembly interactions is demonstrated by macrocyclic host-based chemosensors that co-assemble multiple receptor or reporter elements within the same solution. The majority of reported multi-macrocyclic host systems rely on non-specific amphiphilic aggregation to co-assemble different host classes, allowing for self-adaptable detection of larger peptide biotargets,[27] and the ability to differentiate model proteins,[28] and cell lines.[29] A recent

[a]*Department of Chemistry, University of Victoria, Victoria, BC V8P 5C2, Canada. E-mail: fhof@uvic.ca*

[b]*Centre for Advanced Materials and Related Technology (CAMTEC), University of Victoria, Victoria, BC V8W 2Y2, Canada*

[c]*Institute of Nanotechnology (INT), Karlsruhe Institute of Technology (KIT), Kaiserstraße 12, 76131 Karlsruhe, Germany*

[d]*Canadian Institute for Substance Use Research, University of Victoria, Victoria, BC V8W 2Y2, Canada*

† Electronic supplementary information (ESI) available: Materials and methods, ^{1}H NMR, DFT and PCA. See DOI: https://doi.org/10.1039/d4sc02788d

‡ Equal contribution.

report shows that macrocycles containing different integrated fluorophores have improved discrimination power when they are combined in solution, forming an adaptive network of sensors.[30] Despite these advances, one consistent limitation of supramolecular host chemosensors is they tend to detect only a single class of analyte. The current conceptual framework would have us overcome these limitations through synthesis of new chemosensors, an approach that is often inefficient and incapable of achieving sensing within multi-component mixtures and real-world samples.

Here we present a new concept in which a mixed host chemosensor positions a single dye within a complex system, conferring the ability to generate different kinds of optical responses to hydrophobic, neutral, and cationic analytes. Supramolecular hosts tend to bind one type of guest analyte, therefore limiting the scope and applicability of any host-based sensing approach that relies on one host class.[31] In this work, we overcome this limitation by co-assembling two different classes of macrocyclic hosts, DimerDye sulfonatocalix[4]arenes and cucurbit[*n*]urils, into a single composite mixed host chemosensor (Fig. 1). Key to this conceptual approach is the integration of a dye into the sulfonatocalix[4]arene scaffold, which both facilitates co-assembly and acts as a reporter for all host–host and host–analyte interactions. The equilibrium of any one pre-assembled mixed host chemosensor is poised to go in different directions depending on the nature of the analyte added, producing multi-responsive outputs, where we define multi-responsive as both "giving different photophysical responses to different analytes" and "responding to dissimilar classes of analytes" (Fig. 1b). We prove the benefits of this simple co-assembly approach in an array-based platform through the differentiation of hydrophobic, cationic, neutral and anionic drugs. We then apply these mixed host sensing systems to the highly challenging task of typing illicit drug samples that were collected from people who use drugs. Since these samples come from unregulated supplies they represent a leap forward in sample complexity compared to all prior efforts in our group.[32]

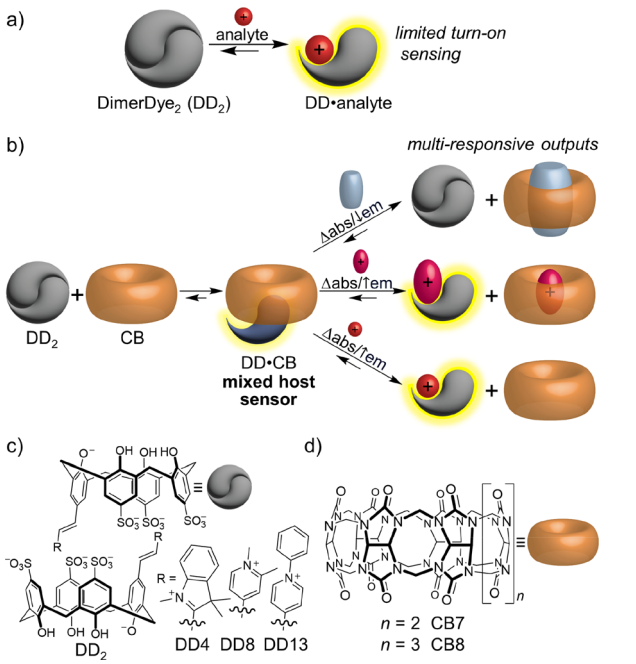

Fig. 1 A mixed host chemosensor produces multi-responsive outputs, increasing the scope of analyte detection. (a) Schematic of DimerDye disassembly-driven turn-on fluorescence sensing of cationic analytes. (b) This work establishes mixed host co-assembled chemosensors that produce multi-responsive outputs for a wide range of hydrophobic, neutral, and cationic analytes. DimerDye complexation with cucurbit[*n*]uril forms a mixed host chemosensor with moderate changes in absorbance/fluorescence. The subsequent addition of an analyte that favors cucurbit[*n*]uril binding produces a change in absorbance and/or turn-off fluorescence, whereas an analyte that prefers DimerDye binding results in a change in absorbance and/or increased fluorescence. The schematic shown represents the expected behaviors for CB7, while additional higher-order complexes are possible for CB8. Structures of (c) DimerDye host chemosensors DD4, DD8, and DD13, and (d) cucurbit[*n*]uril hosts CB7 and CB8 used in this work.

Results and discussion

Design of mixed host chemosensors

Two distinct host classes were selected to encourage host–host co-assembly. Previously reported DimerDye sulfonatocalix[4]arenes DD4, DD8, and DD13 (Fig. 1c),[32] and cucurbit[*n*]uril hosts, CB7 and CB8 (Fig. 1d) were selected to promote hetero co-assembly while contributing different analyte binding properties. Sulfonatocalix[4]arenes contain a flexible chalice-shaped cavity and negatively charged upper rim.[33] In aqueous solution the DimerDye analogs form a homodimer, stacking two fluorophores in an antiparallel quenched arrangement. Upon analyte binding, DimerDyes provide turn-on fluorescence detection through a disassembly-driven sensing mechanism (Fig. 1a).[32,34,35] The selected DimerDyes (DD4, DD8, and DD13) cover a range of structural, absorbance, and emission properties, however, they are limited to binding cationic analytes. Conversely, cucurbit[*n*]utils have a larger range of reported analyte interactions.[36,37] They contain a barrel-shaped rigid nonpolar cavity lined with neutral polar carbonyl portals; reporting strong binding with neutral hydrophobic guests complementary in size and shape,[38,39] and amphiphilic cationic ammonium or diammonium guests that favor hydrophobic and ion–dipole interactions.[36] We selected CB7 and CB8 to accommodate different sized guests, where the larger CB8 cavity offers binding to bulkier hydrophobic drugs.[40,41] We predicted the combination of these two host classes would co-assemble through hydrophobic and ion–dipole interactions from the DimerDye pendant arm binding the cucurbit[*n*]uril cavity and interacting with the polar carbonyl portals.

Mixed host co-assembly sensing mechanism

Different pairs of one DimerDye and one cucurbit[*n*]uril can co-assemble to form a mixed host chemosensor with distinct photophysical properties. Combinations of DD4, DD8 and DD13 with CB7 and CB8 were screened for induced changes in DimerDye absorbance and/or fluorescence (Fig. S9†). The mixed host pairs that displayed significant changes in absorbance

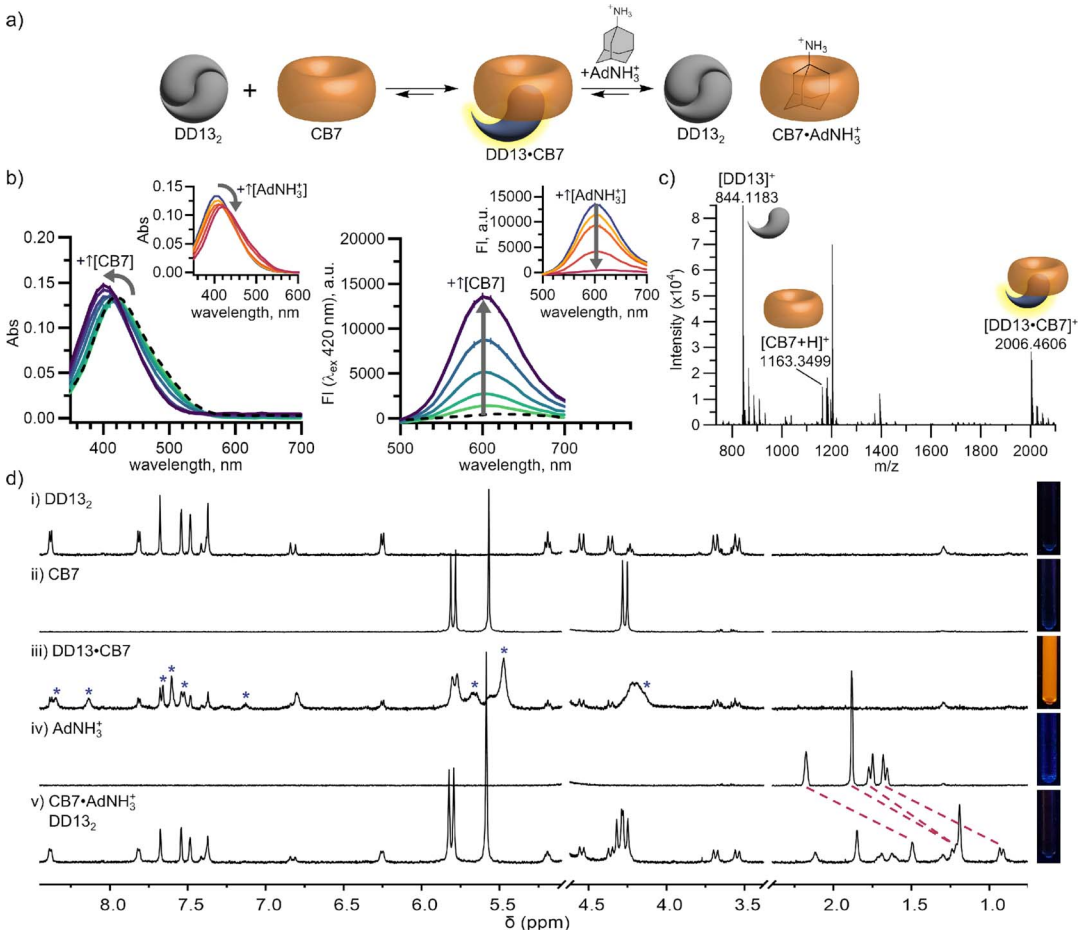

Fig. 2 Mixed host DD13·CB7 co-assembly functions as a turn-off chemosensor for strong binding guests of CB7. (a) Schematic of DD13·CB7 formation and sensing mechanism of $AdNH_3^+$. (b) The addition of increasing concentrations of CB7 (1.3 to 84 μM) into DD13 (10.5 μM) results in a blue shift in absorbance (left) and increased fluorescence (right). Black dashed line represents DD13 (10.5 μM). Insets show the addition of increasing concentrations of $AdNH_3^+$ (2.6 to 21 μM) to the co-assembled DD13·CB7 chemosensor induces a red shift in absorbance (left) and turn-off fluorescence (right). Inset blue line represents DD13 (10.5 μM) with CB7 (21 μM). All samples in NaH_2PO_4/Na_2HPO_4 (10 mM, pH 7.4) in H_2O. (c) MALDI-TOF MS of DD13 (50 μM) with CB7 (50 μM) confirms DD13·CB7 co-assembly. (d) ^1H NMR of (iii) DD13 (100 μM) with CB7 (100 μM) shows evidence of hetero host co-assembly by the appearance of new upfield-shifted DD13 peaks and new CB7 peaks (blue stars). Disassembly of the homodimer $DD13_2$ is supported by the fluorescent appearance of the NMR tube. In (v) the addition of $AdNH_3^+$ (100 μM) displaces the DD13·CB7 complex, indicated by the upfield-shifted $AdNH_3^+$ peaks (red dashed lines) and return of native homodimer $DD13_2$ peaks. The non-fluorescent appearance further supports the reformation of the homodimer $DD13_2$. All samples in NaH_2PO_4/Na_2HPO_4 (10 mM, pD 7.4) in D_2O (500 MHz, 298 K). NMR tubes irradiated with a hand-held UV lamp (λ_{ex} 356 ± 20 nm).

and/or fluorescence (DD4·CB8, DD8·CB8, DD13·CB8, and DD13·CB7) were selected for further study. To establish the formation of these hetero host–host complexes, changes in DimerDye absorbance and emission were monitored during titrations with increasing concentrations of cucurbit[*n*]uril. Titrations of CB8 into DD4 and CB7 into DD13 resulted in both changes in absorbance and turn-on fluorescence (Fig. 2a, b, S10 and S11†). These results indicate the parent DimerDye disassembles from its native homodimer state, with the turn-on fluorescence response strongly supporting the formation of a hetero-complex between the two hosts. Independently, ^1H NMR experiments further support the formation of hetero-complexes DD4·CB8 and DD13·CB7 by the appearance of new upfield-shifted and broadened resonances, attributed to the DimerDye pendant arm protons being in a shielded environment (Fig. 2d, S12 and S13†). The broadened CB7 peaks indicate possible aggregate formation at concentrations used in NMR, coinciding with the low solubilities of these mixed host assemblies (Fig. 2d, S12 and S13†). Upon addition of CB8, the DimerDyes DD8 and DD13, exhibited shifts in absorbance, indicating that CB8 forms a hetero-complex with DD8 and DD13 (Fig. S10 and S11†). However, these complexation events caused minimal changes in emission (Fig. S10†). In cases where both a color change and turn-on emission are observed (DD4·CB8 and DD13·CB7), we suspect the homodimer disassembly is driven by the pendant arm binding to cucurbit[*n*]uril, producing a turn-on fluorescence response. A molecular model of a possible 1 : 1 co-assembly of DD13 with CB7 is presented in Fig. S15.† Matrix-assisted laser desorption ionization-time of flight mass spectrometry (MALDI-TOF MS) further confirmed

1 : 1 complexation, reporting a DD13·CB7 co-assembly peak of *m*/*z* 2006.4606 (Fig. 1c). In cases where only a color change is observed (DD8·CB8 and DD13·CB8) it is evident that hetero-host interactions are occurring. We suspect the non-fluorescent state is a result of assemblies where the DimerDye pendant arms are in a stacked quenched arrangement. These possible complexes include cucurbit[*n*]uril outer-surface binding interactions,[42] where multi-hetero assemblies with sulfonatocalix[4]arenes in aqueous solution have been reported,[43,44] as well as potential ternary complexes in the larger CB8 cavity,[45–47] where two DimerDye pendant arms could potentially bind stacked inside the CB8 cavity. Irrespective of the exact complexes occurring in solution, these co-assemblies constitute different mixed host chemosensors from which distinct absorbance and fluorescence sensing outputs can arise (Fig. 1b).

Mixed host mechanistic studies with a CB-selective guest demonstrate multi-responsive emergent sensing properties that are not present in the parent chemosensor. To validate the contribution of CB's sensing responses, we selected amantadine ($AdNH_3^+$) as a high affinity guest for CB7 (K_d = 240 fM),[48] while the adamantane moiety has been shown to scarcely interact with sulfonated calixarenes.[49] Our ^{1}H NMR experiments corroborate this, showing minimal binding of $AdNH_3^+$ to DD13 (Fig. S14†). In contrast, the addition of $AdNH_3^+$ to the pre-assembled moderately fluorescent co-assembled mixed host chemosensor DD13·CB7 resulted in a turn-off fluorescence response and red-shifted absorbance (Fig. 2b). ^{1}H NMR studies independently confirmed the turn-off fluorescence response is due to the reformation of the quenched homodimer complex $DD13_2$ and assembly of the host–guest complex CB7·$AdNH_3^+$ (Fig. 2d and S13†). These results show that mixed host co-assemblies can produce photophysical responses through analyte binding to the non-fluorophore-containing host, effectively increasing the scope of analyte detection from a single sensing assembly.

Mixed host chemosensors further expand detection capabilities to new classes of analytes. On their own, DimerDyes have been reported to detect cationic illicit drugs.[32] To determine if mixed host chemosensors expand sensing abilities we selected cocaine, cannabidiol (CBD) and Vitamin C as analytes, representing cationic, neutral and anionic classes of drugs (Fig. 3). As a direct comparison, we measured the fluorescence responses of the mixed host chemosensor DD13·CB7 and isolated $DD13_2$ (Fig. 4). Assays with only DimerDyes provided limited information for these drugs, only producing a turn-on fluorescence response to the cationic analyte, cocaine and insignificant responses to the neutral and anionic analytes (Fig. 4b). However, the mixed host chemosensor DD13·CB7 produced varied emergent responses to the different analyte classes; with increased and blue-shifted emission for cationic cocaine, decreased and blue-shifted emission for neutral CBD, and a slight, non-shifted decrease in emission to anionic Vitamin C (Fig. 4a). We probed whether the co-assembly of chemosensors would affect the emission intensities and limits of detection (LODs), using cationic cocaine as a test analyte. The LODs of cocaine with mixed host chemosensors (DD4·CB8, DD8·CB8, DD13·CB8 and DD13·CB7) were of similar magnitude to the parent DimerDyes (DD4, DD8 and DD13), ranging from 0.5 to 3.6 μM (Table S1†). Interestingly, mixed host chemosensors DD4·CB8, DD13·CB8 and DD13·CB7 showed an overall enhancement of fluorescence in comparison to the isolated parent DimerDyes (DD4 and DD13), displaying larger changes in amplitude (Fig. S16–S18†). Although mixed-host systems have competing analyte–host and host–host interactions, these results emphasize favorable emergent

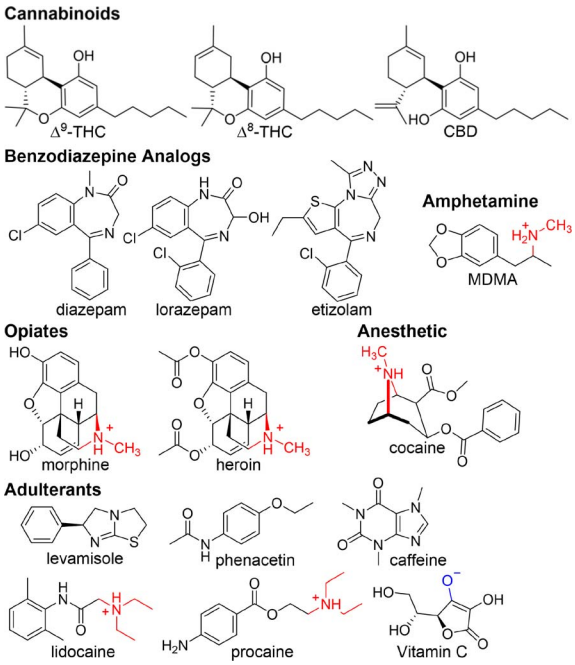

Fig. 3 Chemical structures of illicit drugs and adulterants ranging in hydrophobic, neutral, cationic and anionic properties.

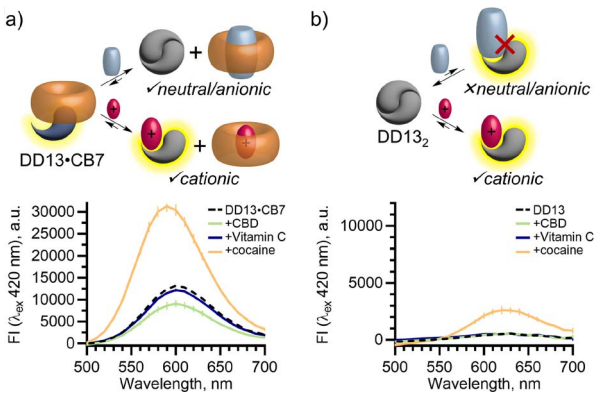

Fig. 4 A mixed host chemosensor has multi-capable responses to neutral, cationic and anionic structures. (a) Fluorescence response of mixed host co-assembled chemosensor DD13·CB7 to anionic Vitamin C, neutral CBD and cationic cocaine. Samples contain [DD13] = 10.5 μM, [CB7] = 21 μM and [drug] = 105 μM. (b) Fluorescence response of isolated DD13 to anionic Vitamin C, neutral CBD and cationic cocaine. Samples contain [DD13] = 10.5 μM and [drug] = 105 μM. All samples are in NaH_2PO_4/Na_2HPO_4 (8.4 mM, pH 7.4) in H_2O with 2% MeOH.

photophysical properties, providing varied responses to different analytes, including those that otherwise wouldn't bind.

Differential sensing

To further probe the power of using mixed host chemosensors, a large set of bulky, hydrophobic, cationic, neutral and anionic drugs and adulterants were selected for differentiation (Fig. 3). The analytes were chosen to test the sensing range capabilities of our mixed host co-assembled chemosensors while targeting compounds commonly found in harm-reduction-based drug checking of Canadian illicit street drugs.[50] An array of mixed host chemosensors (DD4·CB8, DD8·CB8, DD13·CB8, and DD13·CB7) were screened for sensing responses, measuring select absorbance and fluorescence wavelengths (Table S2†). Principal component analysis (PCA) was then used to analyze the fingerprint response patterns, aiming to discriminate samples while minimizing the number of required observations, see ESI† for systematic PCA process.[51]

Mixed host chemosensors can generate surprising emergent properties, including the differentiation of drugs for which neither host is considered to be a canonical binder. Cannabinoids pose a challenge for detection by supramolecular hosts as their neutral structure makes them poor guests. Hooley *et al.* showed that water-soluble deep cavitand sensors bind tetrahydrocannabinol (THC), and can detect and discriminate THC from its metabolites.[52] DimerDyes alone prefer cationic guests and do not give any detectable change in fluorescence response to cannabinoids (Fig. 4b). Although THC has been reported not to bind CB7,[53] we found our mixed host chemosensors DD13·CB7 and DD13·CB8 each produced variable, information-rich responses. We postulate that the decreased emission observed from DD13·CB7 upon addition of CBD (Fig. 4a), is a result of higher-order complexation events that either disrupt mixed host co-assembly or otherwise perturb the emission of the DimerDye fluorophore. Not only was cannabinoid sensing possible from the mixed host chemosensors, but the combination of absorbance and fluorescence outputs from only two mixed host chemosensors in an array (DD13·CB7 and DD13·CB8) allowed for the complete discrimination of highly similar Δ^8- and Δ^9-THC isomers, which differ only in the position of a double bond (Fig. 5a and S19†). These results show that emergent properties are produced from the co-assembly with cucurbit[*n*]uril hosts, providing superior data-rich responses (Fig. 5).

A small array of mixed host chemosensors achieves discrimination of a large set of illicit drugs and adulterants from many distinct chemical classes. We first focused on a test set containing illicit central nervous system depressants, which included both neutral benzodiazepines and cationic opiates. In this analysis, the benzodiazepines etizolam and diazepam displayed overlapping confidence ellipses while the other depressants were discriminated (Fig. 6a and S21†). Next, we studied a test set including cocaine and MDMA, along with a set of pharmacologically active adulterants commonly added for their synergistic effects (Fig. 6b and S22†).[54,55] The prescription

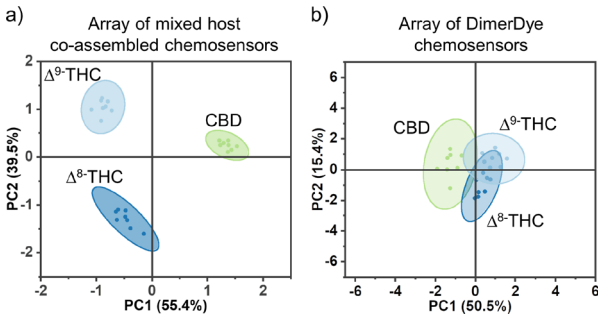

Fig. 5 An array of mixed host chemosensors discriminates highly similar neutral cannabinoids. (a) PCA score plot of a mixed host co-assembled DD·CB sensor array completely discriminates CBD, Δ^8-THC and Δ^9-THC isomers. Sensor array includes absorbance and fluorescence responses of mixed host sensing pairs DD13·CB8 and DD13·CB7. Samples contain [DD] = 10.5 μM, [CB] = 21 μM and [drug] = 105 μM. (b) On their own, DimerDye chemosensors do not discriminate cannabinoids. Sensor array contains absorbance and fluorescence responses of DD4, DD8 and DD13. Samples contain [DD] = 10.5 μM and [drug] = 105 μM. PCA score plots show each sample set (n = 8) enclosed by 95% confidence ellipses. All samples are in NaH_2PO_4/Na_2HPO_4 (8.4 mM, pH 7.4) in H_2O with 2% MeOH.

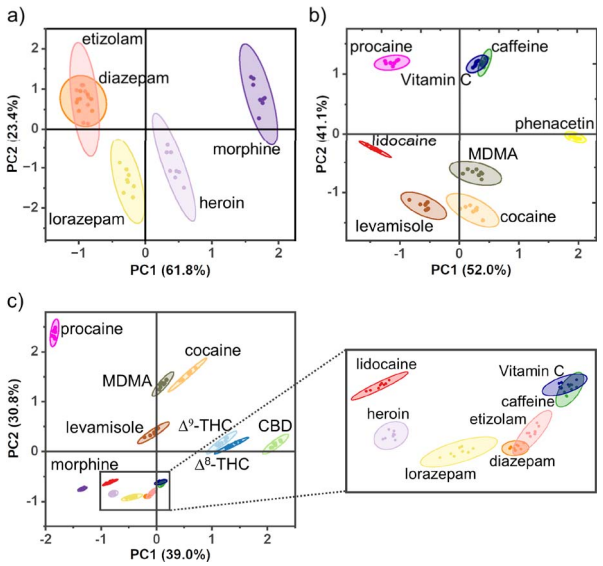

Fig. 6 An array of mixed host co-assembled chemosensors distinguishes between different classes of cationic and neutral illicit drugs and adulterants. (a) PCA analysis of central nervous system depressants; neutral benzodiazepines and cationic opiates. The array of mixed host chemosensors includes absorbance and fluorescence responses from DD8·CB8, DD13·CB8 and DD13·CB7. (b) PCA plot discriminates anesthetics and amphetamine from common adulterants. The array of mixed host chemosensors includes responses from DD4·CB8, DD13·CB8, and DD13·CB7. (c) PCA analysis of all tested drugs and adulterants. The array of mixed host chemosensors includes responses from DD4·CB8, DD8·CB8, DD13·CB8 and DD13·CB7. PCA (correlation) score plot shows each sample set (n = 8) enclosed by 95% confidence ellipses. Samples contain [DD] = 10.5 μM, [CB] = 21 μM and [drug] = 105 μM. All samples are in NaH_2PO_4/Na_2HPO_4 (8.4 mM, pH 7.4) in H_2O with 2% MeOH.

adulterants procaine, lidocaine, levamisole, and phenacetin, were discriminated from the illicit drugs cocaine and MDMA, whereas the adulterants with fewer health repercussions,

Vitamin C and caffeine, overlapped with each other. Lastly, a plot combining all tested drugs maintained similar discrimination patterns among the combined test set, with similar deficiencies in the overlap of two benzodiazepines and the adulterants Vitamin C and caffeine (Fig. 6c and S23†).

Real-world illicit street drug samples represent a challenging set of multi-component targets for identification. Tests that merely reveal the presence or absence of potent substances like fentanyl are less informative tools for harm reduction in the context of the drug overdose crisis.[56] People who use drugs access drug checking services to reduce risks by obtaining an understanding of the complete composition (all active illicit drugs, adulterants, and inert compounds), with specific quantities to assess potency and dangers.[57] Currently, multiple instrument-based techniques are employed, such as combinations of immunoassay test strips, chromatography, mass spectrometry, Raman, and infrared (IR) spectroscopic methods.[58] Typing drug samples using a chemosensor array would provide

Table 1 Multi-component illicit street drug sample composition

Street drug sample	Composition[a]
A	Cocaine (90%), sorbitol
B	Bromazolam (>80% single component)
C	Methylenedioxymethamphetamine (MDMA, >80% single component)
D	Methylenedioxyamphetamine (MDA, 50%), dimethyl sulfone
E	Fentanyl (20%), caffeine, erythritol
F	Fentanyl (13%), fluorofentanyl (1%), caffeine
G	Fentanyl (6%), bromazolam (5%), chloroisobutyryl fentanyl (0.1%), caffeine
H*	Fentanyl (16%), fluorofentanyl (14%), 4-anilino-*N*-phenethyl-piperidine (ANPP, 3.7%), erythritol, caffeine
I*	Fentanyl (18%), fluorofentanyl (16%), ANPP (3.5%), erythritol, caffeine

[a] Street drug samples were acquired through substance, the Vancouver Island Drug Checking Project, located in Victoria, Canada where sample composition was evaluated by FTIR and sample quantification was determined by PS-MS. *Samples H and I were provided by two different people who use drugs reporting the same drug from the same batch and supplier.

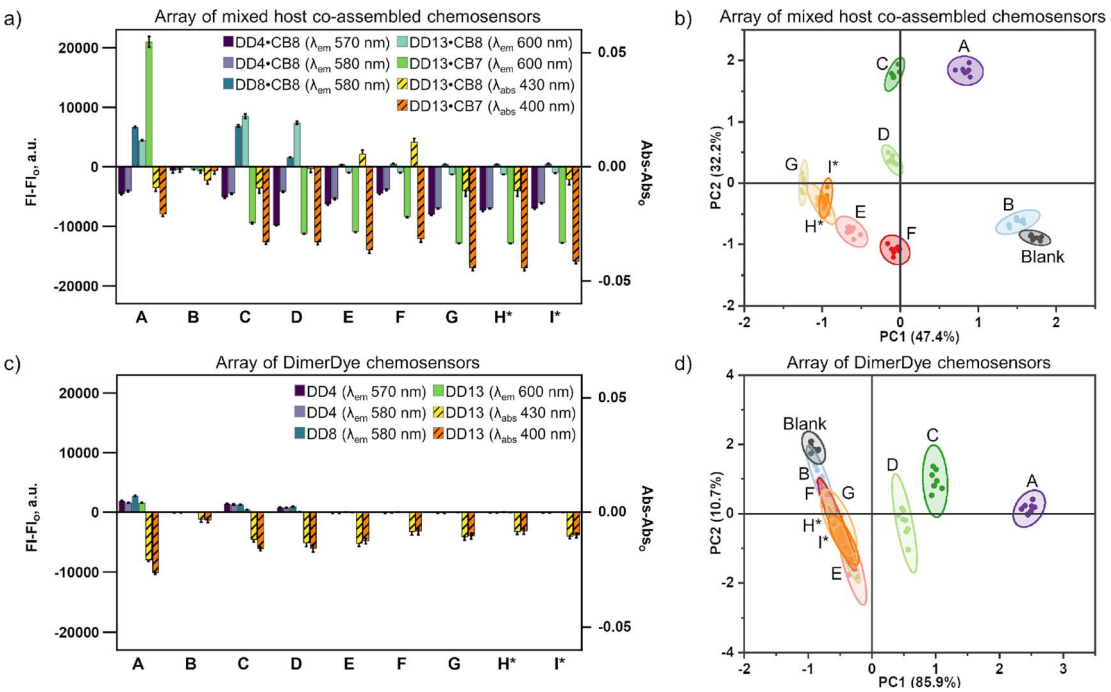

Fig. 7 An array of mixed host co-assembled chemosensors provides data-rich responses that discriminate multi-component street drug samples. (a) An array of mixed host co-assembled chemosensors shows diverse response patterns of absorbance and fluorescence to multi-component street drug samples A–I. (b) PCA analysis using absorbance and fluorescence responses from DD4·CB8, DD8·CB8, DD13·CB8, and DD13·CB7. Samples contain [DD] = 10.5 μM, [CB] = 21 μM and [street drug sample] = 0.03 mg mL^{-1}. (c) An array of DimerDye chemosensors shows similar response patterns of absorbance and fluorescence to multi-component street drug samples A–I. (d) DimerDye chemosensors on their own do not discriminate different multi-component street drug samples. Sensor array contains absorbance and fluorescence responses of DD4, DD8 and DD13. Samples contain [DD] = 10.5 μM and [drug] = 0.03 mg mL^{-1}. PCA score plots show each sample set (n = 8) enclosed by 95% confidence ellipses. All samples are in NaH_2PO_4/Na_2HPO_4 (8.4 mM, pH 7.4) in H_2O with 2% MeOH.

a complementary technique to current instrument-based analysis. Here we aimed to see if our mixed host chemosensors could be applied to illicit multi-component street drug samples to distinguish different composition profiles previously encountered within the drug-checking ecosystem. Street drug samples were provided by people who use drugs through substance, the Vancouver Island Drug Checking Project,[59,60] where drug composition and quantification were determined using Fourier transform infrared (FTIR) spectroscopy and paper spray mass spectrometry (PS-MS) (Table 1 and Fig. S24†). To capture the landscape of street drugs commonly in use in British Columbia, Canada, we studied representative samples from different drug classes (A–E), as well as several fentanyl-containing samples that varied slightly in composition (E–H). We also included two fentanyl samples of the same composition that arrived at the drug-checking site from two distinct users but originating from the same batch and supplier (H and I). Similar to the current protocols used for drug checking, we prepared the street drug samples for sensing experiments dissolving 1.5 mg in 1 mL methanol.[61] These stock solutions were then further diluted down to 0.03 mg mL^{-1} in all sensing experiments.

Mixed host chemosensors identify multi-component street drug samples where a comparable traditional sensor array cannot. Full spectral absorbance and fluorescence responses of each mixed host chemosensor (DD4·CB8, DD8·CB8, DD13·CB8 and DD13·CB7) were acquired for all multi-component street drug samples, to determine if mixed host sensing operated in more complex sample matrices (Fig. S25†). To provide a direct comparison to a traditional sensor array, responses of each isolated DimerDye (DD4, DD8, and DD13) were also collected (Fig. S26†). Mixed host chemosensors provided responses of increased emission to cationic cocaine (A), MDMA (C) and MDA (D) multi-component samples, and varying decreased emission responses to neutral bromazolam (B) and various fentanyl samples (E–I) (Fig. 7a, b and S25†). In comparison, DimerDye chemosensors alone produced sensing responses smaller in amplitude, only providing increased emission responses for cationic samples A, C and D (Fig. 7c, d and S26†). Select absorbance and fluorescence wavelengths from the array of mixed host chemosensors (Table S4†) were applied to PCA analysis, providing discrimination of all multi-component samples (Fig. 7b and S27†). The samples H and I were essentially identical by instrument-based drug checking analysis, having been reported as the same drug from the same supplier (Table 1). The results of the mixed host sensor array overlap, and therefore correctly identify H and I as the same street drug sample. The same observations (Table S5†) were applied to PCA analysis of the isolated DimerDye as a direct comparison of the classical single-host-class sensor array. Only discrimination of cationic samples A, C, and D were achieved, with the remaining samples (B, E–I) overlapping (Fig. 7d and S28†). These results show the combination of multiple host classes introduces useful variability in binding interactions. The information-rich sensing responses provide a dramatic enhancement of the overall performance.

Conclusions

This work shows the value of increased systems chemistry complexity through easily co-assembled mixed host chemosensors. Interconnected equilibria are created by combining multiple binding sites of different inherent affinities within the same sensing solution. In doing so, this approach harnesses simple macrocycle combinations to generate more information-rich sensing fingerprints from a single composite sensing system. This self-assembly-based design provides a facile route to broadening the scope of analytes, where the ability to detect untargeted analytes emerges through unexpected higher-order complexation interactions. This tactic can be easily applied to a wide range of established reporter chromophores, fluorophores, and recognition binding elements, offering almost unlimited possibilities for enhancing current sensing systems.

Data availability

The data that supports the findings of this study is available in the ESI.† The raw experimental data used in PCA analysis have been uploaded as an .exl file.

Author contributions

A. J. S., J. K., F. B. and F. H. conceptualized and visualized the project. A. J. S., J. K. and E. P. contributed methodology. A. J. S. and J. K. contributed investigation. A. J. S., J. K. and F. B. contributed formal analysis. D. H., F. B. and F. H. supervised. F. H. acquired funding. A. J. S. wrote the original draft and all authors contributed to review and editing.

Conflicts of interest

There are no conflicts to declare.

Acknowledgements

The authors thank the Natural Sciences and Engineering Research Council of Canada (NSERC, RGPIN-2019-04806) for financial support. A. J. S. thanks NSERC for the Canadian Graduate Scholarship-Doctoral (CGS-D). J. K. thanks MITACS for the Globalink Research Award. We wish to thank the UVic-Genome BC Proteomics Centre, Victoria, Canada and Angela Jackson for expert assistance on MALDI-TOF MS. We also thank CAMTEC for the use of shared facilities and Dr Cornelia Bohne for helpful discussion.

Notes and references

1 M. Nilam and A. Hennig, Enzyme assays with supramolecular chemosensors – the label-free approach, *RSC Adv.*, 2022, **12**, 10725–10748.
2 J. Krämer, R. Kang, L. M. Grimm, L. De Cola, P. Picchetti and F. Biedermann, Molecular Probes, Chemosensors, and Nanosensors for Optical Detection of Biorelevant

Molecules and Ions in Aqueous Media and Biofluids, *Chem. Rev.*, 2022, **122**, 3459–3636.
3 Y. Geng, W. J. Peveler and V. M. Rotello, Array-based "Chemical Nose" Sensing in Diagnostics and Drug Discovery, *Angew. Chem., Int. Ed.*, 2019, **58**, 5190–5200.
4 L. Guerrini, E. Garcia-Rico, N. Pazos-Perez and R. A. Alvarez-Puebla, Smelling, Seeing, Tasting—Old Senses for New Sensing, *ACS Nano*, 2017, **11**, 5217–5222.
5 L. Motiei and D. Margulies, Molecules That Generate Fingerprints: A New Class of Fluorescent Sensors for Chemical Biology, Medical Diagnosis, and Cryptography, *Acc. Chem. Res.*, 2023, **56**, 1803–1814.
6 B. Rout, L. Unger, G. Armony, M. A. Iron and D. Margulies, Medication Detection by a Combinatorial Fluorescent Molecular Sensor, *Angew. Chem., Int. Ed.*, 2012, **51**, 12477–12481.
7 Z. Pode, R. Peri-Naor, J. M. Georgeson, T. Ilani, V. Kiss, T. Unger, B. Markus, H. M. Barr, L. Motiei and D. Margulies, Protein Recognition by a Pattern-Generating Fluorescent Molecular Probe, *Nat. Nanotechnol.*, 2017, **12**, 1161–1168.
8 M. De, S. Rana, H. Akpinar, O. R. Miranda, R. R. Arvizo, U. H. F. Bunz and V. M. Rotello, Sensing of Proteins in Human Serum Using Conjugates of Nanoparticles and Green Fluorescent Protein, *Nat. Chem.*, 2009, **1**, 461–465.
9 S. Rana, N. D. B. Le, R. Mout, K. Saha, G. Y. Tonga, R. E. S. Bain, O. R. Miranda, C. M. Rotello and V. M. Rotello, A Multichannel Nanosensor for Instantaneous Readout of Cancer Drug Mechanisms, *Nat. Nanotechnol.*, 2015, **10**, 65–69.
10 Y. Geng, J. J. Amante, H. L. Goel, X. Zhang, M. R. Walker, D. C. Luther, A. M. Mercurio and V. M. Rotello, Differentiation of Cancer Stem Cells Through Nanoparticle Surface Engineering, *ACS Nano*, 2020, **14**, 15276–15285.
11 R. Peri-Naor, Z. Pode, N. Lahav-Mankovski, A. Rabinkov, L. Motiei and D. Margulies, Glycoform Differentiation by a Targeted, Self-Assembled, Pattern-Generating Protein Surface Sensor, *J. Am. Chem. Soc.*, 2020, **142**, 15790–15798.
12 Y. C. Pan, J. H. Tian and D. S. Guo, Molecular Recognition with Macrocyclic Receptors for Application in Precision Medicine, *Acc. Chem. Res.*, 2023, **56**, 3626–3639.
13 J. Chen, R. J. Hooley and W. Zhong, Applications of Synthetic Receptors in Bioanalysis and Drug Transport, *Bioconjugate Chem.*, 2022, **33**, 2245–2253.
14 R. Pinalli, A. Pedrini and E. Dalcanale, Biochemical sensing with macrocyclic receptors, *Chem. Soc. Rev.*, 2018, **47**, 7006–7026.
15 B. T. Nguyen and E. V. Anslyn, Indicator–Displacement Assays, *Coord. Chem. Rev.*, 2006, **250**, 3118–3127.
16 A. C. Sedgwick, J. T. Brewster, T. Wu, X. Feng, S. D. Bull, X. Qian, J. L. Sessler, T. D. James, E. V. Anslyn and X. Sun, Indicator displacement assays (IDAs): the past, present and future, *Chem. Soc. Rev.*, 2021, **50**, 9–38.
17 R. N. Dsouza, U. Pischel and W. M. Nau, Fluorescent dyes and their supramolecular host/guest complexes with macrocycles in aqueous solution, *Chem. Rev.*, 2011, **111**, 7941–7980.
18 H. A. Fargher, S. D'Oelsnitz, D. J. Diaz and E. V. Anslyn, Pushing Differential Sensing Further: The Next Steps in Design and Analysis of Bio-Inspired Cross-Reactive Arrays, *Analysis Sensing*, 2023, **3**, e202200095.
19 Y. Mei, Q. W. Zhang, Q. Gu, Z. Liu, X. He and Y. Tian, Pillar[5]arene-Based Fluorescent Sensor Array for Biosensing of Intracellular Multi-neurotransmitters through Host–Guest Recognitions, *J. Am. Chem. Soc.*, 2022, **144**, 2351–2359.
20 C. Hu, T. Jochmann, P. Chakraborty, M. Neumaier, P. A. Levkin, M. M. Kappes and F. Biedermann, Further Dimensions for Sensing in Biofluids: Distinguishing Bioorganic Analytes by the Salt-Induced Adaptation of a Cucurbit[7]uril-Based Chemosensor, *J. Am. Chem. Soc.*, 2022, **144**, 13084–13095.
21 J. Chen, B. L. Hickey, Z. Gao, A. A. P. Raz, R. J. Hooley and W. Zhong, Sensing Base Modifications in Non-Canonically Folded DNA with an Optimized Host:Guest Sensing Array, *ACS Sens.*, 2022, **7**, 2164–2169.
22 J. Chen, A. D. Gill, B. L. Hickey, Z. Gao, X. Cui, R. J. Hooley and W. Zhong, Machine learning aids classification and discrimination of noncanonical DNA folding motifs by an arrayed host:guest sensing system, *J. Am. Chem. Soc.*, 2021, **143**, 12791–12799.
23 J. Chen, B. L. Hickey, L. Wang, J. Lee, A. D. Gill, A. Favero, R. Pinalli, E. Dalcanale, R. J. Hooley and W. Zhong, Selective discrimination and classification of G-quadruplex structures with a host–guest sensing array, *Nat. Chem.*, 2021, **13**, 488–495.
24 B. L. Hickey, J. Chen, Y. Zou, A. D. Gill, W. Zhong, J. G. Millar and R. J. Hooley, Enantioselective Sensing of Insect Pheromones in Water, *Chem. Commun.*, 2021, **57**, 13341–13344.
25 B. Wang, J. Han, N. M. Bojanowski, M. Bender, C. Ma, K. Seehafer, A. Herrmann and U. H. F. Bunz, An Optimized Sensor Array Identifies All Natural Amino Acids, *ACS Sens.*, 2018, **3**, 1562–1568.
26 N. D. Saha, S. Pradhan, R. Sasmal, A. Sarkar, C. M. Berač, J. C. Kölsch, M. Pahwa, S. Show, Y. Rozenholc, Z. Topçu, V. Alessandrini, J. Guibourdenche, V. Tsatsaris, N. Gagey-Eilstein and S. S. Agasti, Cucurbit[7]uril Macrocyclic Sensors for Optical Fingerprinting: Predicting Protein Structural Changes to Identifying Disease-Specific Amyloid Assemblies, *J. Am. Chem. Soc.*, 2022, **144**, 14363–14379.
27 Z. Xu, S. Jia, W. Wang, Z. Yuan, B. J. Ravoo and D. S. Guo, Heteromultivalent Peptide Recognition by Co-assembly of Cyclodextrin and Calixarene Amphiphiles Enables Inhibition of Amyloid Fibrillation, *Nat. Chem.*, 2019, **11**, 86–93.
28 J. H. Tian, X. Y. Hu, Z. Y. Hu, H. W. Tian, J. J. Li, Y. C. Pan, H. B. Li and D. S. Guo, A Facile Way to Construct Sensor Array Library *via* Supramolecular Chemistry for Discriminating Complex Systems, *Nat. Commun.*, 2022, **13**, 4293.
29 X. Y. Hu, Z. Y. Hu, J. H. Tian, L. Shi, F. Ding, H. B. Li and D. S. Guo, A Heteromultivalent Host-Guest Sensor Array for Cell Recognition and Discrimination, *Chem. Commun.*, 2022, **58**, 13198–13201.

30 A. J. Selinger and F. Hof, Adaptive Supramolecular Networks: Emergent Sensing from Complex Systems, *Angew. Chem., Int. Ed.*, 2023, **62**, e202312407.
31 W. Zhong and R. J. Hooley, Combining Excellent Selectivity with Broad Target Scope: Biosensing with Arrayed Deep Cavitand Hosts, *Acc. Chem. Res.*, 2022, **55**, 1035–1046.
32 M. A. Beatty, A. J. Selinger, Y. Li and F. Hof, Parallel Synthesis and Screening of Supramolecular Chemosensors that Achieve Fluorescent Turn-on Detection of Drugs in Saliva, *J. Am. Chem. Soc.*, 2019, **141**, 16763–16771.
33 D. S. Guo, K. Wang and Y. Liu, Selective Binding Behaviors of *p*-Sulfonatocalixarenes in Aqueous Solution, *J. Inclusion Phenom. Macrocyclic Chem.*, 2008, **62**, 1–21.
34 M. A. Beatty, J. Borges-González, N. J. Sinclair, A. T. Pye and F. Hof, Analyte-Driven Disassembly and Turn-On Fluorescent Sensing in Competitive Biological Media, *J. Am. Chem. Soc.*, 2018, **140**, 3500–3504.
35 C. Gallo, S. S. Thomas, A. J. Selinger, F. Hof and C. Bohne, Mechanism of a Disassembly-Driven Sensing System Studied by Stopped-Flow Kinetics, *J. Org. Chem.*, 2021, **86**, 10782–10787.
36 S. J. Barrow, S. Kasera, M. J. Rowland, J. del Barrio and O. A. Scherman, Cucurbituril-Based Molecular Recognition, *Chem. Rev.*, 2015, **115**, 12320–12406.
37 S. Sinn and F. Biedermann, Chemical Sensors Based on Cucurbit[*n*]uril Macrocycles, *Isr. J. Chem.*, 2018, **58**, 357–412.
38 K. I. Assaf and W. M. Nau, Cucurbiturils: from Synthesis to High-affinity Binding and Catalysis, *Chem. Soc. Rev.*, 2015, **44**, 394–418.
39 A. I. Lazar, F. Biedermann, K. R. Mustafina, K. I. Assaf, A. Hennig and W. M. Nau, Nanomolar Binding of Steroids to Cucurbit[*n*]urils: Selectivity and Applications, *J. Am. Chem. Soc.*, 2016, **138**, 13022–13029.
40 S. Murkli, J. Klemm, A. T. Brockett, M. Shuster, V. Briken, M. R. Roesch and L. Isaacs, *In Vitro* and *In Vivo* Sequestration of Phencyclidine by Me_4Cucurbit[8]uril, *Chem.–Eur. J.*, 2021, **27**, 3098–3105.
41 D. Das, K. I. Assaf and W. M. Nau, Applications of Cucurbiturils in Medicinal Chemistry and Chemical Biology, *Front. Chem.*, 2019, **7**, 619.
42 Y. Huang, R. H. Gao, M. Liu, L. X. Chen, X. L. Ni, X. Xiao, H. Cong, Q. J. Zhu, K. Chen and Z. Tao, Cucurbit[*n*]uril-Based Supramolecular Frameworks Assembled Through Outer-Surface Interactions, *Angew. Chem., Int. Ed.*, 2021, **60**, 15166–15191.
43 X. Tian, L. X. Chen, Y. Q. Yao, K. Chen, M. D. Chen, X. Zeng and Z. Tao, 4-Sulfocalix[4]arene/Cucurbit[7]uril-Based Supramolecular Assemblies Through the Outer Surface Interactions of Cucurbit[*n*]uril, *ACS Omega*, 2018, **3**, 6665–6672.
44 R. G. Lin, L. S. Long, R. B. Huang and L. S. Zheng, Directing Role of Hydrophobic−Hydrophobic and Hydrophilic−Hydrophilic Interactions in the Self-Assembly of Calixarenes/Cucurbiturils-Based Architectures, *Cryst. Growth Des.*, 2008, **8**, 791–794.
45 J. Liu, H. Lambert, Y. W. Zhang and T. C. Lee, Rapid Estimation of Binding Constants for Cucurbit[8]uril Ternary Complexes Using Electrochemistry, *Anal. Chem.*, 2021, **93**, 4223–4230.
46 F. Biedermann, I. Ross and O. A. Scherman, Host–guest accelerated photodimerisation of anthracene-labeled macromolecules in water, *Polym. Chem.*, 2014, **5**, 5375–5382.
47 M. Sayed, F. Biedermann, V. D. Uzunova, K. I. Assaf, A. C. Bhasikuttan, H. Pal, W. M. Nau and J. Mohanty, Triple emission from *p*-dimethylaminobenzonitrile-cucurbit[8]uril triggers the elusive excimer emission, *Chem.–Eur. J.*, 2015, **21**, 691–696.
48 S. Liu, C. Ruspic, P. Mukhopadhyay, S. Chakrabarti, P. Y. Zavalij and L. Isaacs, The Cucurbit[*n*]uril Family: Prime Components for Self-Sorting Systems, *J. Am. Chem. Soc.*, 2005, **127**, 15959–15967.
49 H. X. Zhao, D. S. Guo, L. H. Wang, H. Qian and Y. Liu, A Novel Supramolecular Ternary Polymer with Two Orthogonal Host–guest Interactions, *Chem. Commun.*, 2012, **48**, 11319–11321.
50 L. Belzak and J. Halverson, Evidence synthesis - The opioid crisis in Canada: a national perspective, *Health Promot. Chronic Dis. Prev. Can.*, 2018, **38**, 224–233.
51 S. Stewart, M. A. Ivy and E. V. Anslyn, The use of principal component analysis and discriminant analysis in differential sensing routines, *Chem. Soc. Rev.*, 2014, **43**, 70–84.
52 A. D. Gill, B. L. Hickey, W. Zhong and R. J. Hooley, Selective Sensing of THC and Related Metabolites in Biofluids by Host:Guest Arrays, *Chem. Commun.*, 2020, **56**, 4352–4355.
53 X. Du, H. Hao, A. Qin and B. Z. Tang, Highly Sensitive Chemosensor for Detection of Methamphetamine by the Combination of AIE Luminogen and Cucurbit[7]uril, *Dyes Pigm.*, 2020, **180**, 108413.
54 C. Cole, L. Jones, J. McVeigh, A. Kicman, Q. Syed and M. Bellis, Adulterants in illicit drugs: a review of empirical evidence, *Drug Test. Anal.*, 2011, **3**, 89–96.
55 L. J. C. Cole, J. McVeigh, A. Kicman, Q. Syed and M. A. Bellis, *Cut: a guide to adulterants, bulking agents and other contaminants found in illicit drugs*, Liverpool John Moores University, Liverpool, 2010.
56 J. C. Halifax, L. Lim, D. Ciccarone and K. L. Lynch, Testing the test strips: laboratory performance of fentanyl test strips, *Harm Reduct. J.*, 2024, **21**, 14.
57 A. Ivsins, J. Boyd, L. Beletsky and R. McNeil, Tackling the Overdose Crisis: The Role of Safe Supply, *Int. J. Drug Pol.*, 2020, **80**, 102769.
58 L. Gozdzialski, B. Wallace and D. Hore, Point-of-care Community Drug Checking Technologies: an Insider Look at the Scientific Principles and Practical Considerations, *Harm Reduct. J.*, 2023, **20**, 39.
59 B. Wallace, R. Hills, J. Rothwell, D. Kumar, I. Garber, T. Van Roode, A. Larnder, F. Pagan, J. Aasen, J. Weatherston, L. Gozdzialski, M. Ramsay, P. Burek, M. S. Azam, B. Pauly, M. A. Storey and D. Hore, Implementing an integrated multi-technology platform for drug checking: Social, scientific, and technological considerations, *Drug Test. Anal.*, 2021, **13**, 734–746.

60 B. Wallace, L. Gozdzialski, A. Qbaich, A. Shafiul, P. Burek, A. Hutchison, T. Teal, R. Louw, C. Kielty, D. Robinson, B. Moa, M. A. Storey, C. Gill and D. Hore, A distributed model to expand the reach of drug checking, *Drugs Habits Soc. Pol.*, 2022, **23**, 220–231.

61 S. A. Borden, A. Saatchi, G. W. Vandergrift, J. Palaty, M. Lysyshyn and C. G. Gill, A New Quantitative Drug Checking Technology for Harm Reduction: Pilot Study in Vancouver, Canada Using Paper Spray Mass Spectrometry, *Drug Alcohol Rev.*, 2022, **41**, 410–418.